

# Photocatalytic reduction of Cr(VI) over different TiO<sub>2</sub> photocatalysts and the effects of dissolved organic species

Limin Wang, Nan Wang, Lihua Zhu\*, Hongwei Yu, Heqing Tang\*

Department of Chemistry and Chemical Engineering, Hubei Key Laboratory of Bioinorganic Chemistry and Materia Medica, Huazhong University of Science and Technology, Wuhan 430074, PR China

Received 11 December 2006; received in revised form 6 April 2007; accepted 13 June 2007

Available online 23 June 2007

## Abstract

The toxic Cr(VI) in industrial wastewaters can be removed by a reduction from Cr(VI) to Cr(III) and a followed precipitation treatment. The reduction of Cr(VI) to Cr(III) is able to be achieved by a photocatalytic process. Thus, photocatalytic reduction of Cr(VI) over TiO<sub>2</sub> catalysts was investigated in both the absence and presence of organic compounds. The TiO<sub>2</sub> catalyst was pre-calcined at different temperatures to tune the photocatalytic activity and surface area of the photocatalyst. Under the tested conditions, the photocatalytic reduction of Cr(VI) behaved as a pseudo-first-order reaction in kinetics. In the absence of any organic species, the rate constant ( $k_{Cr}$ ) for the photocatalytic reduction of Cr(VI) was found to be increased initially, passing a maximum, and then decreased, as calcination temperature was increased. In the presence of organic compounds, however,  $k_{Cr}$  was decreased with the increase of calcination temperature. A marked synergistic effect between the photocatalytic reduction of Cr(VI) and organic compounds was observed over the photocatalyst with the largest specific surface area. These results demonstrated that the photocatalytic reduction of Cr(VI) alone was dependent on both of specific surface area and crystalline structure of the photocatalyst in the absence of any organic compounds, but was dominated by the specific surface area of the photocatalyst in the presence of organic compounds because of the synergistic effect between the photocatalytic reduction of Cr(IV) and the photocatalytic oxidation of organic compounds.

© 2007 Elsevier B.V. All rights reserved.

**Keywords:** TiO<sub>2</sub>; Photocatalysis; Hexavalent chromium; Organic pollutants; Synergistic effect

## 1. Introduction

Semiconductor photocatalysis has been intensively investigated for its application to environmental pollutants degradation. It has been found that a variety of organic and inorganic pollutants can be oxidized or reduced by photogenerated holes and electrons over semiconductors [1]. Of all semiconductors, TiO<sub>2</sub> is the most widely investigated one because of its favorable chemical property, high stability and low cost. Since heterogeneous photocatalytic reactions take place on the surface, the surface properties of TiO<sub>2</sub> such as surface hydroxyl groups, surface area, particle size, crystalline phase, surface defects and surface metal deposits play a critical role in determining the efficiencies and mechanisms of the photocatalytic reaction. TiO<sub>2</sub> surfaces have been actively modified through manipulating the

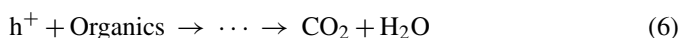
above parameters in order to improve the photocatalytic activity [2–8]. Liu et al. [2] reported enhancement of photocatalytic activity of silver-loaded TiO<sub>2</sub>, and found that deposited silver on TiO<sub>2</sub> surface acts as a site where electrons accumulate, leading to better separation between electrons and holes on the modified TiO<sub>2</sub> surface. Toyoda et al. [3] observed the crystallinity of anatase was an important factor in order to get high photocatalytic activity for the decomposition of methylene blue in water. Our group have recently observed the activity of TiO<sub>2</sub> toward the photocatalytic degradation of azo dye and phenols is significantly enhanced by coating a thin layer of polyaniline [4], a layer of molecular imprinted polymer [5], and by in situ surface modification via adsorption of cupric and fluoride ions [6]. Navío et al. [7] found that the activity is dependent on not only the structural differences but also the type of redox reaction involved. Lu et al. [8] investigated the enhancement of  $\beta$ -cyclodextrin on TiO<sub>2</sub> photocatalytic oxidation of azo dyes and reduction of Cr(VI) in aqueous solutions, and proposed the mechanism as the formation of complexes of  $\beta$ -cyclodextrin with the dyes and Cr(VI) anions on the TiO<sub>2</sub> surface.

\* Corresponding author. Tel.: +86 27 87543432; fax: +86 27 87543632.

E-mail addresses: [lh Zhu63@yahoo.com.cn](mailto:lh Zhu63@yahoo.com.cn) (L. Zhu), [hqtang62@yahoo.com.cn](mailto:hqtang62@yahoo.com.cn) (H. Tang).

Recently, increasing attention has been paid to the photocatalytic reduction of inorganic contaminants. The application of the TiO<sub>2</sub> photocatalytic reduction process is reported to effectively remove various toxic metal ions, such as Hg(II) [9,10], Se(IV) [11], Se(VI) [12,13], Cd(II) [14,15], Zn(II) [14], Cu(II) [16,17] and Cr(VI) [18–20]. Here, the photocatalytic system cannot be used directly to remove a toxic metal from a wastewater, but should be followed by an effective separation method (e.g. precipitation) for the reduced forms of the metal. Cr(VI) is a toxic, carcinogenic and mobile contaminant originating from industrial processes such as electroplating, pigment production, leather tanning, or paint manufacture. Its concentration in water is necessarily restricted to be less than 0.05 ppm by the environmental quality standards for water pollution control. The preferred treatment is reduction of Cr(VI) to the less harmful Cr(III), which can be precipitated in neutral or alkaline solutions as Cr(OH)<sub>3</sub> [21,22].

The photo-reduction of Cr(VI) to Cr(III) can be achieved via a photocatalytic process with a simplified mechanism as follows:



UV light illumination on TiO<sub>2</sub> produces hole–electron pairs (reaction (1)) at the surface of the photocatalyst. After the hole–electron pairs being separated, the electrons can reduce Cr(VI) to Cr(III) (reaction (2)), and the holes may lead to generation of O<sub>2</sub> in the absence of any organics (reaction (3)). Therefore, in a completely inorganic aqueous solution, the net photocatalytic reaction is the three-electron-reduction of Cr(VI) to Cr(III) with oxidation of water to oxygen, which is a kinetically slow four-electron process [23,24]. And hence the photocatalytic reduction of Cr(VI) alone is quite slow. Alternatively, the photocatalytic reduction of Cr(VI) can be carried out in couple with the photocatalytic oxidation of organic pollutants by adding some amount of organic pollutants in solution. In the presence of degradable organic pollutants, the holes can produce  $\bullet\text{OH}$  radicals (reaction (4)), which can further degrade the organics to CO<sub>2</sub> and H<sub>2</sub>O (reaction (5)). Of course, the holes can also directly oxidize the organic molecules (reaction (6)). In other words, in the presence of organic species, the photogenerated holes are rapidly scavenged from the TiO<sub>2</sub> particles, suppressing electron–hole recombination on TiO<sub>2</sub> and accelerating the reduction of Cr(VI) by photogenerated electron [25]. One of the important strategies of promoting the photocatalytic reduction of Cr(VI) (and the photocatalytic degradation of organic pollutants) is enhancing the charge separation, which can be achieved by improving the structure of the photocatalyst and by introducing scavengers of holes and/or electrons in the solution. It has been reported that the presence of organic species as sacrificial electron donor can accelerate the photocatalytic reduction

of Cr(VI) [26–28]. However, it is yet unknown how the nature of the TiO<sub>2</sub> photocatalyst influences the reduction of Cr(VI) coupled with photocatalytic oxidation of organic pollutants, and what is the key point of selecting a TiO<sub>2</sub> photocatalyst being suitable for coupled photocatalytic degradation of inorganic and organic pollutants. In the present work, therefore, the photocatalytic reduction of Cr(VI) was systematically investigated over anatase-type TiO<sub>2</sub> catalysts in the absence and presence of organic species, where the TiO<sub>2</sub> photocatalysts were pre-calcined to possess different crystallinity and specific surface areas.

## 2. Experimental

Commercial anatase-type TiO<sub>2</sub> nanoparticles (referred to as A000) were obtained from Zhoushan Nano Company, and P25 nanopowders were supplied by Degussa. To obtain TiO<sub>2</sub> photocatalysts with different crystalline phases, the A000 nanoparticles were calcined in air for 2 h at temperatures of 200, 400, 500, 600, 700, 800 and 900 °C, respectively. The resultant catalysts were accordingly referred to as A200, A400, A500, A600, A700, A800 and A900. All other chemicals were of analytical reagent grade, and were used as received. Distilled water was used to prepare of all solutions. Cr(VI) stock solution (0.02 mol L<sup>-1</sup>) was prepared by dissolving K<sub>2</sub>Cr<sub>2</sub>O<sub>7</sub> into distilled water.

Photocatalytic experiments were carried out in a 150 mL reactor at room temperature (25 ± 2 °C). For all photocatalytic runs, 100 mL solution containing 0.4 mmol L<sup>-1</sup> Cr(VI) with or without the addition of organic compounds was maintained in suspension by a magnetic stirrer. In each experiment, the catalyst was suspended with a load of 1 g L<sup>-1</sup>, the solution pH was adjusted to pH 2.0 with H<sub>2</sub>SO<sub>4</sub> solutions, and the concentration of the organic compound, if added, was 0.4 mmol L<sup>-1</sup> except for formic acid (4.35 mmol L<sup>-1</sup>). A 20-W UV lamp with a maximum emission at 253.7 nm was positioned about 10 cm above the photo-reactor. Prior to irradiation, the suspension was ultrasonicated for 1 min and magnetically stirred for 30 min in dark to ensure adsorption–desorption equilibration. The concentration of Cr(VI) after equilibration was measured and taken as the initial concentration (c<sub>0</sub>), to discount the adsorption in the dark.

During the given time intervals, 2 mL of solution was taken from the suspension and centrifuged at 14,000 rpm for 15 min to remove TiO<sub>2</sub> nanoparticles. The concentration of Cr(VI) after illumination (c<sub>t</sub>) was determined spectrophotometrically by measuring the absorbance at 349 nm on a Cary 50 UV–vis spectrophotometer (Varian). When salicylic acid was used as a organic pollutant, the Cr(VI) concentration was analyzed by diphenylcarbazide photometric method at 540 nm, which can effectively diminish the interference from the absorption of salicylic acid and its degradation intermediates. Concentration of phenol was obtained with a PU-2089 high-performance liquid chromatographer (JASCO), equipped with a C18 ODS column. The detection wavelength was 270 nm, and the effluent consists of a mixture of water and methanol (65:35). At least duplicated runs were carried out for each condition.

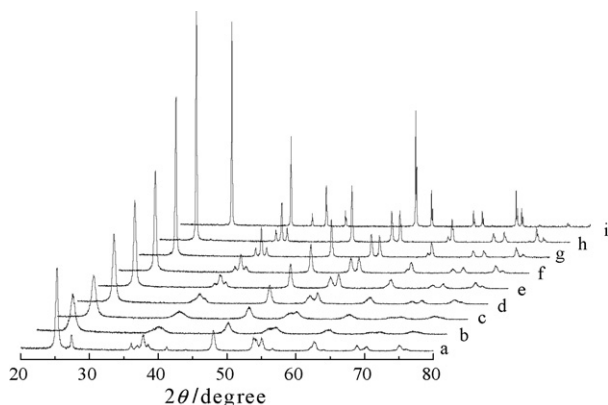


Fig. 1. XRD patterns of P25 (a) and  $\text{TiO}_2$  nanoparticles before (b) and after being calcined for 2 h at 200 °C (c), 400 °C (d), 500 °C (e), 600 °C (f), 700 °C (g), 800 °C (h), and 900 °C (i).

In order to determine the amount of Cr(VI) adsorbed on different catalysts, 0.3 g of catalyst was dispersed and stirred with a magnetic stirrer in 100 mL of 0.4 mmol L<sup>-1</sup> Cr(VI) with and without the addition of organic compounds for an hour in the dark. After centrifuging, the concentration of Cr(VI) was analyzed in the same way as mentioned above.

The crystalline structure of the photocatalyst was investigated by using X-ray diffraction (XRD) technique. The XRD patterns were obtained by using an X'Pert PRO X-ray diffractometer (PANalytical) with a Cu K $\alpha$  radiation source. The accelerating voltage and the applied current were 40 kV and 40 mA, respectively. The Brunauer–Emmett–Teller (BET) surface area was determined via low-temperature N<sub>2</sub> adsorption–desorption experiments by using a micrometrics ASAP2020 automated apparatus. All samples were degassed for 3 h at 353 K before the analysis. The specific surface area was calculated using the BET method based on the N<sub>2</sub> adsorption isotherm.

### 3. Results and discussion

#### 3.1. Crystalline structure and specific surface area of photocatalysts

It is known that the preparation of efficient  $\text{TiO}_2$  photocatalyst via a sol–gel process requires a calcination treatment to achieve an appropriate crystalline structure. XRD analysis was made for  $\text{TiO}_2$  nanoparticles A000 before and after being calcined, together with P25 as a control. As shown in Fig. 1, P25 shows well-defined diffraction peaks corresponding to a phase mixture of anatase and rutile (curve a), where the anatase peak appears at  $2\theta = 25.4^\circ$  and the rutile peak at  $27.5^\circ$  [29,30]. The intensity

ratio of the main diffraction peak for anatase at  $2\theta = 25.4^\circ$  to that for rutile at  $27.5^\circ$  is evaluated as 80:20 approximately. The  $\text{TiO}_2$  nanoparticles from Zhoushan (A000) have a structure of pure anatase (curve b), but a rather amorphous diffraction pattern with wider peaks was observed for the powders without heat treatment, indicating poorer crystallinity. When A000 was calcined, a higher calcination temperature was generally favorable to the improvement of the crystallinity of  $\text{TiO}_2$  powders. As calcination temperature was increased from 200 to 800 °C, the peak at  $2\theta = 25.4^\circ$  increased in intensity along with sharpening of the peak (curves c–h), demonstrating a pure anatase structure with improved crystallinity. At a temperature as high as 900 °C, the peak at  $25.4^\circ$  disappeared, and the peak at  $27.5^\circ$  was observed instead (curve i). This suggests that the phase transforms completely from anatase to rutile structure at this temperature, which is in agreement with that the phase change from anatase to rutile ranges from 600 to 1100 °C, depending on the preparation conditions [31].

Specific surface area is one of the important properties of photocatalyst. A greater specific surface area is generally favorable to yielding a higher photocatalytic activity. As-received A000 has a BET specific surface area as high as 180.9 m<sup>2</sup> g<sup>-1</sup>. After it is calcined, its specific surface area becomes smaller generally with increasing of calcination temperature as shown in Table 1. For example, after being calcined at 200, 500 and 700 °C, the specific surface area is rapidly decreased from initial 180.9–145.2, 63.2 and 15.9 m<sup>2</sup> g<sup>-1</sup>, respectively. For a comparison, the BET surface area of P25 was measured as 49.6 m<sup>2</sup> g<sup>-1</sup>, approaching to the values of A500 and A600.

#### 3.2. Photocatalytic reduction of Cr(VI) in the absence and presence of organics

At first, it was experimentally found that the chemical reduction of Cr(VI) in both the absence and the presence of organic compounds was negligible when the Cr(VI) solution was not irradiated with UV light or no  $\text{TiO}_2$  catalyst was added into the solution. For example, a 120-min UV irradiation converted only 0.2% of the added Cr(VI) in the absence of  $\text{TiO}_2$  photocatalyst, and a 120-min treatment in the presence of  $\text{TiO}_2$  but without the UV illumination produced a conversion of less than 0.9% for Cr(VI). This means that both the direct photolysis and chemical reduction of Cr(VI) are negligible.

Then, the kinetics of the photocatalytic reduction of Cr(VI) were investigated. As shown in Fig. 2, the kinetic data obtained for the Cr(VI) reduction over A000 in both the absence and the presence of organic compounds can be fitted to a rate expression of a pseudo-first-order reaction:  $\ln(c_t/c_0) = -k_{Cr}t$ , where  $c_0$

Table 1  
BET surface areas of photocatalysts

	Catalyst					
	A000	A200	A500	A600	A700	Degussa P25
Crystal phase	Anatase	Anatase	Anatase	Anatase	Anatase	Anatase/rutile = 4/1
Surface area (m <sup>2</sup> g <sup>-1</sup> )	180.9	145.2	63.2	39.7	15.9	49.6

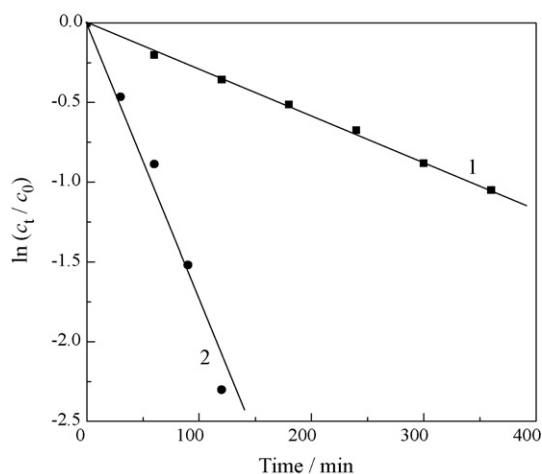


Fig. 2. Kinetic data for the photocatalytic reduction of Cr(VI) over A000 in the absence (1) and presence (2) of formic acid.

and  $c_t$  represent the Cr(VI) concentrations before and after the irradiation,  $t$  is the irradiation time, and  $k_{Cr}$  is the apparent rate constant of the photocatalytic reduction of Cr(VI) as a pseudo-first-order reaction. It is seen from Fig. 2 that the addition of formic acid significantly enhances the photocatalytic reduction of Cr(VI). By alternating the organic compounds, the kinetics of the photocatalytic reduction of Cr(VI) were further investigated over different photocatalysts. Under normal conditions in our work, the photocatalytic reduction of Cr(VI) over each of the used photocatalysts was observed to exhibit the kinetics of a pseudo-first-order reaction in both the absence and presence of the organic compounds. Therefore,  $k_{Cr}$  is able to be used for evaluating the effects of some factors on the photocatalytic reduction of Cr(VI).

Fig. 3 shows the dependence of  $k_{Cr}$  in the absence of any organics over different TiO<sub>2</sub> photocatalysts. As calcination temperature is increased, the rate constant of photocatalytic reduction of Cr(VI) increases initially, passes a maximum at 500 °C, then decreases rapidly. It is interesting that the calcination at 500 °C yields photocatalytic activity as high as P25

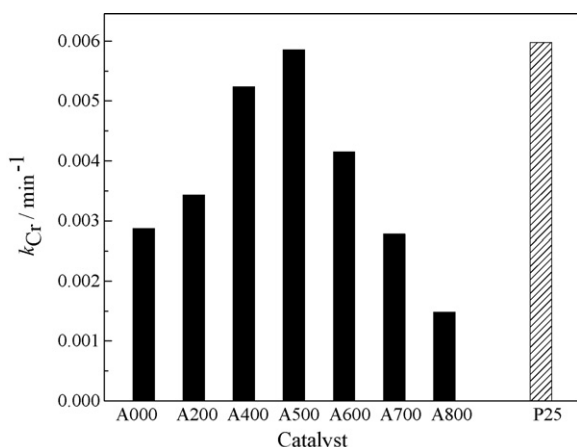


Fig. 3. Values of the apparent rate constant  $k_{Cr}$  of photocatalytic reduction of Cr(VI) in the absence of any organics over different TiO<sub>2</sub> photocatalysts.

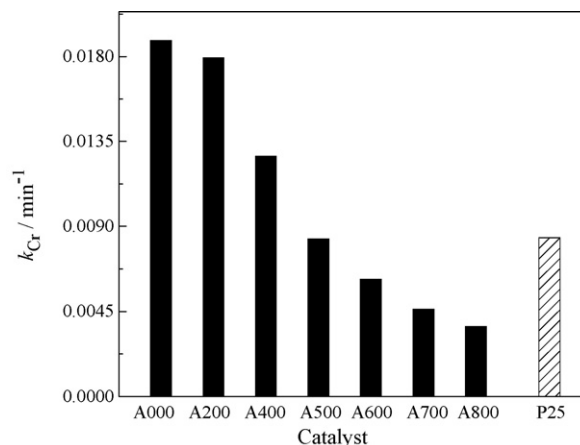


Fig. 4. Values of the apparent rate constant  $k_{Cr}$  of photocatalytic reduction of Cr(VI) in the presence of formic acid over different TiO<sub>2</sub> photocatalysts.

toward the photocatalytic reduction of Cr(VI) in the absence of any organics.

Fig. 4 represents the values of  $k_{Cr}$  in the presence of formic acid over different TiO<sub>2</sub> catalysts. By comparing with Fig. 3, we can conclude that the photocatalytic reduction of Cr(VI) is generally accelerated by adding formic acid into the Cr(VI) solution, which is in agreement of the observations on the literature [26–28]. For the catalyst A000 without the calcination treatment, the addition of formic acid increases the value of  $k_{Cr}$  from 0.00287 to 0.01886 min<sup>-1</sup> with a factor of about 6.6 times. As the calcination temperature is increased, the values of  $k_{Cr}$  are decreased in the presence of formic acid, although most of which are correspondingly greater than that in the absence of formic acid. Being similar to the case in the absence of any organics, the rate constant for A500 (calcined at 500 °C) was almost the same as that for P25 in the presence of formic acid.

In order to further investigate the effect of organics on the photocatalytic reduction of Cr(VI), citric acid, salicylic acid, *p*-hydroxybenzoic acid and phenol were used instead of formic acid. Table 2 tabulates the values of  $k_{Cr}$  obtained in the presence of different organic compounds. In spite of different organic compounds, the rate constant of the photocatalytic reduction of Cr(VI) over A500 (TiO<sub>2</sub> calcined at 500 °C) was found to be nearly the same as that of P25. Table 2 reveals again that A000 is

Table 2

Values of the apparent rate constant  $k_{Cr}$  of photocatalytic reduction of Cr(VI) obtained in the presence of different organic compounds

Organic compound	$k_{Cr}$ (min <sup>-1</sup> )		
	A000	A500	P25
Blank	0.00287	0.00586	0.00598
Formic acid	0.01886 (6.6) <sup>a</sup>	0.00837 (1.4)	0.00841 (1.4)
Citric acid	0.06058 (21.1)	0.02412 (4.1)	0.02439 (4.1)
Salicylic acid	0.02742 (9.6)	0.01302 (2.2)	0.01267 (2.1)
<i>p</i> -Hydroxybenzoic acid	0.01097 (3.8)	0.00637 (1.1)	0.00646 (1.1)
Phenol	0.01583 (5.5)	0.00902 (1.5)	0.00870 (1.4)

<sup>a</sup> The values in the parentheses are the ratio of  $k_{Cr}$  in the presence of the organics to that in the absence of any organics.

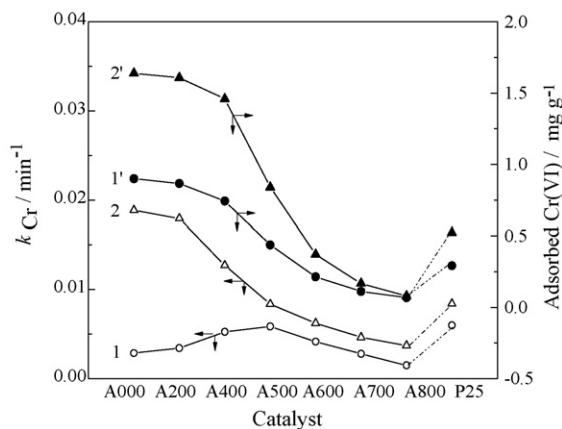


Fig. 5. Values of the apparent rate constant  $k_{Cr}$  (1, 2) and the dark adsorption (1', 2') of Cr(VI) in the absence (1, 1') and presence (2, 2') of formic acid over different TiO<sub>2</sub> catalysts. The lines are only for guidance of eye light.

the best photocatalyst for the photocatalytic reduction of Cr(VI) in the presence of organic compounds, and it also demonstrates that the addition of any of the tested organic compounds can significantly promote the photocatalytic reduction of Cr(VI) over A000. The enhancing effect of the added organics is observed to be dependent on nature of added organic compounds. As can be seen,  $k_{Cr}$  in the presence of different organics increases in the following order: *p*-hydroxybenzoic acid < phenol < formic acid < salicylic acid < citric acid, being roughly consistent with that reported by Prairie et al. [32]. Of the tested organics, addition of citric acid is the most efficient, increasing  $k_{Cr}$  from 0.00287 to 0.06058 min<sup>-1</sup> by a factor of 21.1 relative to that in the absence of organics.

### 3.3. A comparison between $k_{Cr}$ and the adsorption of Cr(VI) over different photocatalysts

Adsorption process plays an important role in photocatalytic reaction [33]. Thus, Fig. 5 compares the photocatalytic activity of the catalyst and the dark adsorption of Cr(VI) in the absence and presence of formic acid over various catalysts. In the absence of formic acid, the dark adsorption of Cr(VI) decreases with increasing calcination temperature (curve 1), while  $k_{Cr}$  first increases and then decreases (curve 1'), reaching a maximum at 500 °C, which was almost the same as that over P25. Because the change tendency of  $k_{Cr}$  value (curve 1) is rather different from that of the adsorption of Cr(VI) (curve 1') when the calcination temperature is lower than 500 °C, we can conclude that the photocatalytic reduction of Cr(VI) is not governed by the adsorption step of Cr(VI) over TiO<sub>2</sub> catalysts in the absence of any organics.

In the presence of formic acid, however, both  $k_{Cr}$  and the dark adsorption of Cr(VI) over TiO<sub>2</sub> catalysts are decreased as calcination temperature is increased. The same change tendency for  $k_{Cr}$  (curve 2) and the Cr(VI) adsorption (curve 2') may suggest that the photocatalytic reduction of Cr(VI) is governed by the adsorption step of Cr(VI) over TiO<sub>2</sub> catalysts in the presence of formic acid, which is general for other tested organics.

Table 3

Values of the apparent rate constant  $k_{phenol}$  of photocatalytic oxidation of phenol in the absence and presence of Cr(VI) over TiO<sub>2</sub>

Catalyst	$k_{phenol}$ (min <sup>-1</sup> )	
	Phenol alone	Phenol + Cr(VI)
A000	0.00195	0.01066
A500	0.00604	0.00527
P25	0.00734	0.00564

### 3.4. Photocatalytic oxidation of phenol by adding Cr(VI) over different TiO<sub>2</sub> photocatalysts

We have also monitored the photocatalytic oxidation of the present organic compounds in our experiment. For the tested organic compounds in the present work, all their photocatalytic oxidation over TiO<sub>2</sub> catalysts has been observed to behave like a pseudo-first-order reaction in kinetics. Thus, we can also use the apparent rate constant  $k_{organic}$  to evaluate the variations in the photocatalytic activity of the photocatalysts toward the oxidation of the organic compounds. Table 3 gives values of the apparent rate constants  $k_{phenol}$  of photocatalytic oxidation of phenol in the absence and presence of Cr(VI) over TiO<sub>2</sub> catalysts. The photocatalytic oxidation of phenol over P25 and A500 is slightly hindered by adding Cr(VI), which is similar to the observation reported on the literature [34]. However, the addition of Cr(VI) increases the apparent rate constant  $k_{phenol}$  of photocatalytic oxidation of phenol over A000 from 0.00195 to 0.01066 min<sup>-1</sup> with a factor of about 5.5 times. From Table 2, we can know that the addition of phenol increases the apparent rate constant  $k_{Cr}$  of photocatalytic reduction of Cr(VI) over A000 from 0.00287 to 0.01583 min<sup>-1</sup> with a factor of about 5.5 times. Such a great synergistic effect between the photocatalytic reduction of Cr(VI) and the oxidation of organic compounds are very exciting from the view point of the photocatalytic treatment of organic and inorganic waste waters. If we appropriately select the photocatalyst, the photocatalytic efficiency can be increased greatly by using a simultaneous photocatalytic reduction of Cr(VI) and the oxidation of organic compounds.

### 3.5. Synergistic effect in coupled photocatalytic degradation of Cr(VI) and organic pollutants

As described in Section 1, the mechanism the photo-reduction of Cr(VI) over TiO<sub>2</sub> may follow a general mechanism being composed of reactions (1)–(6). In this mechanism, the presence of Cr(VI) may enhance the photocatalytic oxidation of organic pollutants, and the addition of organic pollutants may promote the photocatalytic reduction of Cr(VI) to Cr(III).

P25 is known as one of the best TiO<sub>2</sub> photocatalysts and used frequently as a benchmark in photocatalysis. It exhibits high activity because of the interaction of anatase and rutile phases in its TiO<sub>2</sub> particles, which enhances the electron–hole separation and increases the total photoefficiency [35,36]. Therefore, P25 yields the highest photocatalytic activity toward the Cr(VI) reduction in the absence of any organics (Fig. 3), and fairly high (although not the highest) photocatalytic activity in the pres-

ence of organic compounds (Fig. 4 and Table 2). In general, adding some organic compounds into the solution is favorable to further increasing of the charge separation by scavenging holes via reactions (4)–(6). But the further increasing is not expected to be so great for P25 because it originally provides efficient charge separation. This is confirmed in Table 2, which shows that the addition of the organic compounds increases  $k_{Cr}$  by only a factor of 1.1–4.1. As for the influence of adding Cr(VI) on the photocatalytic oxidation of organic compounds, the enhancing effect is also much less efficient over P25. In the case of photocatalytic oxidation of phenol, the addition of Cr(VI) as electron scavengers even decreases  $k_{phenol}$  slightly (Table 3). This deceleration of phenol oxidation may be attributed to catalyst deactivation in the presence of Cr(VI) [34]. In our opinion, because the charge separation over P25 is efficient and the generation of  $O_2^{\bullet-}$  radicals ( $O_2 + e^- \rightarrow O_2^{\bullet-}$ ;  $O_2^{\bullet-} + H^+ \rightarrow \bullet OH$ ) is fast in acidic solutions, the addition of Cr(VI) as electron scavengers could not considerably promote the charge separation. Under this condition, competitive adsorption of Cr(VI) may decrease the adsorption of phenol molecules on the surface of P25 particles, resulting in a deceleration of the phenol oxidation. Therefore, P25 is not a good photocatalyst for treatment of organic waste water in coupled with Cr(VI)-containing inorganic waste water, because this combination will not produce a marked synergistic effect in the photo-degradation of both the specified organic and inorganic pollutants.

Beside the crystalline structure, the specific surface area is another important factor influencing the  $TiO_2$ 's activity. In general, better anatase phase and greater surface area are favorable to higher photocatalytic activity. Heat treatment will change both the crystalline structure and specific surface area of the photocatalyst, leading to a complicate effect of calcination temperature on the photocatalytic activity of  $TiO_2$  (Figs. 3 and 4). Before the heat treatment, catalyst A000 has a rather poorer crystalline structure of anatase phase, along with a very large specific surface area of  $180.9 \text{ m}^2 \text{ g}^{-1}$ . For the heat treated photocatalysts, the crystallinity of anatase phase is improved (Fig. 1), but the specific surface area is decreased (Table 1) as calcination temperature is increased. When calcination temperature is lower than  $500^\circ\text{C}$ , the improvement in the crystallinity of anatase phase is more important, resulting in an increased  $k_{Cr}$  for higher calcination temperature in the absence of organics; When calcination temperature is higher than  $500^\circ\text{C}$ , the decreased specific surface area dominates the photo-reduction of Cr(VI), leading to a decreased  $k_{Cr}$  for higher calcination temperature in the absence of any organics (Fig. 3). Because of the reversed effects of the two factors, the  $500^\circ\text{C}$  calcination yields the best photocatalyst (A500), being as excellent as P25.

Unlike in P25, there is no anatase/rutile structure in A000. The charge separation in A000 and the calcined photocatalysts should be not so efficient as in P25. The addition of organic compounds as hole scavengers will favor to promoting the charge separation and accelerating the photo-reduction of Cr(VI) over such photocatalysts. As experimentally observed, the addition of organic compounds significantly enhances the photo-reduction

of Cr(VI) over A000 (Fig. 4 and Table 2), increasing  $k_{Cr}$  value by a factor of 6.6 times in the presence of formic acid. In this case, therefore, the specific surface area is more important than the crystalline structure of the photocatalyst in the photocatalytic reduction of Cr(VI). This is further supported by the observation that related to the value of  $k_{Cr}$  in the absence of any organics, the addition of the tested organics can increased  $k_{Cr}$  by a factor of about 4–21 over A000 (Table 2), being much greater than that over P25.

When the calcinations temperature is increased, the BET specific surface area of the photocatalyst becomes smaller, leading to a decreased dark adsorption of Cr(VI). Because the enhanced Cr(VI) reduction requires a rapid proceeding of the photocatalytic oxidation of organics in parallel, a smaller specific surface area is unfavorable to the Cr(VI) reduction. This accounts for the fact that in the presence of organic compounds,  $k_{Cr}$  is decreased as calcination temperature is increased. The dominant role of the surface area is further supported by the observation that both A500 and P25 display similar photocatalytic activities for the reduction of Cr(VI) because their BET surface area are comparable to each other, although their crystalline structures are very different. Our observations are similar to that reported by Colón et al. [34] and Siemon et al. [37], who found that Hombikat UV100 (with a surface area being ca. 5 times of that of P25) performed better than P25 for the photoreduction of Cr(VI) in the presence of salicylic acid [34] and EDTA [37].

#### 4. Conclusions

It was confirmed that the photocatalytic reduction of Cr(VI) is influenced by the nature of  $TiO_2$  photocatalysts. The effects of the photocatalysts' nature on the photocatalytic reduction of Cr(VI) is further dependent on the existence of photocatalytic oxidizable organics. In the absence of any organic compounds, the photocatalytic reduction of Cr(VI) alone is dependent on both specific surface area and crystallinity of the photocatalyst. In the presence of appropriate organic compounds, however, the photocatalytic reduction of Cr(VI) couple with the photo-oxidation of the added organics, leading to a great promotion of the photocatalytic reduction of Cr(VI) due to the significant synergistic effect of photocatalytic treatment of Cr(VI) and organic pollutants. This synergistic effect is increased with increase of the BET specific surface area of  $TiO_2$  photocatalyst, being less dependent on its crystalline structure. Therefore, the  $TiO_2$  photocatalyst (A000) having the largest specific surface area among the tested photocatalysts has been observed to show the best activity for the photocatalytic reduction of Cr(VI) in the presence of organic compounds, increasing the reduction rates of Cr(VI) by more than 20 times in the presence of citric acid, relative to the reduction of Cr(VI) alone. These findings indicate that the photocatalytic reduction of Cr(VI) alone requires the use of  $TiO_2$  photocatalysts with a appropriate combination of crystalline structure and specific surface area, and a simultaneous photocatalytic treatment of inorganic Cr(VI) and organic pollutants needs the use of  $TiO_2$  photocatalysts with a large specific surface area.

## Acknowledgements

The generous financial support by the National Science Foundation of China (Nos. 30571536 and 20677019) was gratefully acknowledged. The Center of Analysis and Testing of Huazhong University of Science and Technology is thanked for characterizing photocatalysts.

## References

- [1] D. Chen, A.K. Ray, Removal of toxic metal ions from wastewater by semiconductor photocatalysis, *Chem. Eng. Sci.* 56 (2001) 1561–1570.
- [2] S.X. Liu, Z.P. Qu, X.W. Han, C.L. Sun, A mechanism for enhanced photocatalytic activity of silver-loaded titanium dioxide, *Catal. Today* 93–95 (2004) 877–884.
- [3] M. Toyoda, Y. Nanbu, Y. Nakazawa, M. Hirano, M. Inagaki, Effect of crystallinity of anatase on photoactivity for methylene blue decomposition in water, *Appl. Catal. B: Environ.* 49 (2004) 227–232.
- [4] J. Li, L. Zhu, Y. Wu, Y. Harima, A. Zhang, H. Tang, Hybrid composites of conductive polyaniline and nanocrystalline titanium oxide prepared via self-assembling and graft polymerization, *Polymer* 47 (2006) 7361–7367.
- [5] X. Shen, L. Zhu, J. Li, H. Tang, Synthesis of molecular imprinted polymer coated photocatalysts with high selectivity, *Chem. Commun.* (2007) 1163–1165.
- [6] N. Wang, Z. Chen, L. Zhu, X. Jiang, B. Lv, H. Tang, Synergistic effects of cupric and fluoride ions on photocatalytic degradation of phenol, *J. Photochem. Photobiol. A: Chem.* 191 (2007) 193–200.
- [7] J.A. Navío, G. Colón, M. Trillas, J. Peral, X. Domènech, J.J. Testa, J. Padrón, D. Rodríguez, M.I. Litter, Heterogeneous photocatalytic reactions of nitrite oxidation and Cr(VI) reduction on iron-doped titania prepared by the wet impregnation method, *Appl. Catal. B: Environ.* 16 (1998) 187–196.
- [8] P. Lu, F. Wu, N. Deng, Enhancement of TiO<sub>2</sub> photocatalytic redox ability by  $\beta$ -cyclodextrin in suspended solutions, *Appl. Catal. B: Environ.* 53 (2004) 87–93.
- [9] L.B. Khalil, M.W. Rophael, W.E. Mourad, The removal of the toxic Hg(II) salts from water by photocatalysis, *Appl. Catal. B: Environ.* 36 (2002) 125–130.
- [10] X. Wang, S.O. Pehkonen, A.K. Ray, Photocatalytic reduction of Hg(II) on two commercial TiO<sub>2</sub> catalysts, *Electrochim. Acta* 49 (2004) 1435–1444.
- [11] T. Tan, D. Beydoun, R. Amal, Effects of organic hole scavengers on the photocatalytic reduction of selenium anions, *J. Photochem. Photobiol. A: Chem.* 159 (2003) 273–280.
- [12] T.T.Y. Tan, D. Beydoun, R. Amal, Photocatalytic reduction of Se(VI) in aqueous solutions in UV/TiO<sub>2</sub> system: kinetic modeling and reaction mechanism, *J. Phys. Chem. B* 107 (2003) 4296–4303.
- [13] T.T.Y. Tan, D. Beydoun, R. Amal, Photocatalytic reduction of Se(VI) in aqueous solutions in UV/TiO<sub>2</sub> system: importance of optimum ratio of reactants on TiO<sub>2</sub> surface, *J. Mol. Catal. A: Chem.* 202 (2003) 73–85.
- [14] C.R. Chenthamarakshan, K. Rajeshwar, Photocatalytic reduction of divalent zinc and cadmium ions in aqueous TiO<sub>2</sub> suspensions: an interfacial induced adsorption–reduction pathway mediated by formate ions, *Electrochim. Commun.* 2 (2000) 527–530.
- [15] V.N.H. Nguyen, R. Amal, D. Beydoun, Effect of formate and methanol on photoreduction/removal of toxic cadmium ions using TiO<sub>2</sub> semiconductor as photocatalyst, *Chem. Eng. Sci.* 58 (2003) 4429–4439.
- [16] S. Yamazaki, S. Iwai, J. Yano, H. Taniguchi, Kinetic studies of reductive deposition of copper(II) ions photoassisted by titanium dioxide, *J. Phys. Chem. A* 105 (2001) 11285–11290.
- [17] T. Kanki, H. Yoneda, N. Sano, A. Toyoda, C. Nagai, Photocatalytic reduction and deposition of metallic ions in aqueous phase, *Chem. Eng. J.* 97 (2004) 77–81.
- [18] Y. Ku, I. Jung, Photocatalytic reduction of Cr(VI) in aqueous solutions by UV irradiation with the presence of titanium dioxide, *Water Res.* 35 (2001) 135–142.
- [19] C.R. Chenthamarakshan, K. Rajeshwar, E.J. Wolfrum, Heterogeneous photocatalytic reduction of Cr(VI) in UV-irradiated titania suspensions: effect of protons, ammonium ions, and other interfacial aspects, *Langmuir* 16 (2000) 2715–2721.
- [20] S. Tuprakay, W. Liengcharernsit, Lifetime and regeneration of immobilized titania for photocatalytic removal of aqueous hexavalent chromium, *J. Hazard. Mater.* B124 (2005) 53–58.
- [21] L.B. Khalil, W.E. Mourad, M.W. Rophael, Photocatalytic reduction of environmental pollutant Cr(VI) over some semiconductors under UV/visible light illumination, *Appl. Catal. B: Environ.* 17 (1998) 267–273.
- [22] D.P. Das, K. Parida, B.R. De, Photocatalytic reduction of hexavalent chromium in aqueous solution over titania pillared zirconium phosphate and titanium phosphate under solar radiation, *J. Mol. Catal. A: Chem.* 245 (2006) 217–224.
- [23] J.J. Testa, M.A. Grella, M.I. Litter, Experimental evidence in favor of an initial one-electron-transfer process in the heterogeneous photocatalytic reduction of chromium(VI) over TiO<sub>2</sub>, *Langmuir* 17 (2001) 3515–3517.
- [24] S.G. Schrank, H.J. José, R.F.P.M. Moreira, Simultaneous photocatalytic Cr(VI) reduction and dye oxidation in a TiO<sub>2</sub> slurry reactor, *J. Photochem. Photobiol. A: Chem.* 147 (2002) 71–76.
- [25] G. Colón, M.C. Hidalgo, J.A. Navío, Influence of carboxylic acid on the photocatalytic reduction of Cr(VI) using commercial TiO<sub>2</sub>, *Langmuir* 17 (2001) 7174–7177.
- [26] J.J. Testa, M.A. Grella, M.I. Litter, Heterogeneous photocatalytic reduction of chromium(VI) over TiO<sub>2</sub> particles in the presence of oxalate: involvement of Cr(V) species, *Environ. Sci. Technol.* 38 (2004) 1589–1594.
- [27] B. Sun, E.P. Reddy, P.G. Smirniotis, Visible light Cr(VI) reduction and organic chemical oxidation by TiO<sub>2</sub> photocatalysis, *Environ. Sci. Technol.* 39 (2005) 6251–6259.
- [28] H. Fu, G. Lu, S. Li, Adsorption and photo-induced reduction of Cr(VI) ion in Cr(VI)-4CP (4-chlorophenol) aqueous system in the presence of TiO<sub>2</sub> as photocatalyst, *J. Photochem. Photobiol. A: Chem.* 114 (1998) 81–88.
- [29] Q. Zhang, L. Gao, J. Guo, Effects of calcination on the photocatalytic properties of nanosized TiO<sub>2</sub> powders prepared by TiCl<sub>4</sub> hydrolysis, *Appl. Catal. B: Environ.* 26 (2000) 207–215.
- [30] J.C. Yu, J. Yu, W. Ho, Z. Jiang, L. Zhang, Effects of F<sup>-</sup> doping on the photocatalytic activity and microstructures of nanocrystalline TiO<sub>2</sub> powders, *Chem. Mater.* 14 (2002) 3808–3816.
- [31] J. Ovenstone, K. Yanagisawa, Effect of hydrothermal treatment of amorphous titania on the phase change from anatase to rutile during calcination, *Chem. Mater.* 11 (1999) 2770–2774.
- [32] M.R. Prairie, L.R. Evans, B.M. Stange, S.L. Martinez, An investigation of TiO<sub>2</sub> photocatalysis for the treatment of water contaminated with metals and organic chemicals, *Environ. Sci. Technol.* 27 (1993) 1776–1782.
- [33] P. Mohapatra, S.K. Samantaray, K. Parida, Photocatalytic reduction of hexavalent chromium in aqueous solution over sulphate modified titania, *J. Photochem. Photobiol. A: Chem.* 170 (2005) 189–194.
- [34] G. Colón, M.C. Hidalgo, J.A. Navío, Photocatalytic deactivation of commercial TiO<sub>2</sub> samples during simultaneous photoreduction of Cr(VI) and photooxidation of salicylic acid, *J. Photochem. Photobiol. A: Chem.* 138 (2001) 79–85.
- [35] B. Sun, A.V. Vorontsov, P.G. Smirniotis, Role of platinum deposited on TiO<sub>2</sub> in phenol photocatalytic oxidation, *Langmuir* 19 (2003) 3151–3156.
- [36] D.C. Hurum, A.G. Agrios, K.A. Gray, T. Rajh, M.C. Thurnauer, Explaining the enhanced photocatalytic activity of Degussa P25 mixed-phase TiO<sub>2</sub> using EPR, *J. Phys. Chem. B* 107 (2003) 4545–4549.
- [37] U. Siemon, D. Bahnemann, J.J. Testa, D. Rodríguez, M.I. Litter, N. Bruno, Heterogeneous photocatalytic reactions comparing TiO<sub>2</sub> and Pt/TiO<sub>2</sub>, *J. Photochem. Photobiol. A: Chem.* 148 (2002) 247–255.